Wu et al., Aerosol and Air Quality Research, Vol. 4, No. 1, pp. 74-90, 2004

Control of Elemental Mercury Vapor in Combustion Systems Using Fe_2O_3 Nanoparticles

Scott Borderieux[1], Chang-Yu Wu[1*], Jean-Claude Bonzongo[1] and Kevin Powers[2]

University of Florida

[1]Department of Environmental Engineering Sciences

[2]Particle Engineering Research Center

Abstract

The U.S. Environmental Protection Agency (EPA) has proposed initial regulations to control mercury (Hg) emissions from coal-burning utilities, the primary source of airborne Hg emissions in the United States. Promising new techniques in capturing Hg involve transformation of elemental Hg into a product that is much more easily collected using conventional air pollution collection devices. In this study, the removal ability of high surface area iron oxide (Fe_2O_3) nanoparticles prepared on solid glass beads by a dry mechanical coating process was examined. The experimental results showed different mechanisms responsible for the removal depending on the air composition. In pure air, the Fe_2O_3 nanoparticles adsorbed and desorbed, while in the presence of nitrogen dioxide (NO_2) they took on a catalytic role. The maximum specific capacity observed in this study was 1528 μg Hg/g Fe_2O_3. This study also identified the effective temperature range (180 – 320 ^oC) for Hg removal, with the optimal temperature being ~260 ^oC. The study reveals the important role of metal oxides in Hg chemistry in combustion systems through heterogeneous oxidation, and demonstrates the potential of Fe_2O_3 nanoparticles as an alternative material to traditional control techniques, such as activated carbon for reducing Hg emissions from incinerators.

Keywords: Mercury, Metal Oxide, Catalyst, Adsorption, NO_2

1. Introduction

Among the various environmental problems today, mercury emission from combustion sources is a major concern. When emitted into the atmosphere, it settles into the soils and waterways where microorganisms, mainly sulfate-reducing bacteria, convert it to methyl-Hg that is readily bioaccumulated and biomagnified through the food chain. In humans, methyl-Hg causes neurological

* Corresponding author. Tel.: 352-392-0845; Fax 352-392-3076.

E-*mail address:* cywu@ufl.edu

damage, and has been shown to cause subtle decrements in motor skills and sensory ability at low doses (the U.S. Environmental Protection Agency [EPA] reference dose with no anticipated risk is 0.1μg/kg of body weight/day), as well as tremors, the inability to walk, and death at high doses (0.1-0.5 μg/g of body weight/day in lab animals; U.S. EPA, 1997). It is especially toxic to a developing fetus. The impact on human health results in higher medical costs and, consequently, in higher insurance premiums. High mercury levels in fish have also resulted in a ban on the consumption of fish caught in several places, including the Everglades and the Great Lakes, which translates into significant economic losses. Recently, the U.S. Food and Drug Administration (FDA) and EPA have issued a joint advisory on fish consumption for mothers and children because of mercury contamination (U.S. EPA, 2004a). The impact on human health, the environment, and the economy clearly speaks for the importance of controlling mercury emissions. As such, U.S. EPA has proposed initial regulations in 2004, with planned implementation in 2010, to control mercury emissions from coal-burning utilities, the primary source of airborne mercury emissions in the United States (U.S. EPA, 2004b).

Due to its unique closed-shell electronic structure ($5d^{10}6s^2$) that is isoelectronic to He ($1S^2$) (Haberland et al., 1993), mercury exists as an elemental vapor at temperatures normally associated with combustion processes. Although some oxidation is thermodynamically favored at the pollution control device inlet (Wu and Biswas, 1993), in real systems the thermodynamically favored products are not formed as a result of frozen equilibrium below about 800 K (Senior et al., 2000). Hence, elemental mercury is present in combustion flue gas and is usually released into the atmosphere. Several stack sampling studies have shown that a high fraction of the mercury emitted from coal-fired power plants, in some cases over 95%, is in elemental form (Bergström, 1986; Meij, 1991). In this elemental form, it is neither water-soluble nor a particle, and therefore difficult to be collected in wet scrubbers or conventional particle control devices such as electrostatic precipitators (ESP) or baghouses. Currently, activated carbon is the most commonly researched material, especially when doped with sulfur or chloride (Krishnan et al., 1994; Zeng et al., 2004). However, the limitation of activated carbon (e.g., significantly increased burden to baghouses, making flyash unsellable) is calling for the development of alternative technology.

Promising new techniques in capturing mercury involve the transformation of mercury, such as through oxidation. Oxidized forms of mercury, usually reported as Hg^{2+} species, are much more easily collected using traditional control devices because they become more water soluble and are better adsorbed on particles. There are many studies on the homogeneous oxidation of mercury in the gas phase. Several researchers (Otani et al., 1988; Hall et al., 1991; Niksa et al., 2001; Lee et al., 2002; Norton et al., 2003) have shown the importance of chlorine species and NO_x. However, the discrepancies (Senior et al., 2000; Niksa et al., 2002) between predicted results for homogeneous oxidation and the actual amount of oxidation that occurs in a system, especially at lower temperatures (below 500 ˚C), show the important role of heterogeneous oxidation as well. Particles can catalyze many reactions that are not expected or seen in particle-free systems. In a coal combustion system, fly

ash is always present. The surface chemistry on the fly ash greatly complicates the analysis of mercury oxidation. Lee et al. (2001) and Norton et al. (2003) indicated that the surface area of unburned carbon in their fly ash was a major factor in their system. Fujiwara et al. (2002) pointed out that the amount of unburned carbon is the determining factor in reported extents of oxidation. Senior et al. (2000) proposed that below 400 ˚C, Cl_2 can be catalytically generated in the presence of particulate matter according to the Deacon process:

$$2HCl + 1/2O_2 \xrightarrow{\text{Particulate Matter}} Cl_2 + H_2O \quad (1)$$

This Cl_2 will then lead to more oxidation.

Besides surface area, the makeup of the particles also is important in the heterogeneous oxidation studies. Lee et al. (2001) and Ghorishi et al. (1999) showed that iron oxide (Fe_2O_3) and copper oxide (CuO) concentrations in fly ash greatly affect the oxidation potential of the system. Norton et al. (2003) disagreed, finding that different fly ashes, including those enriched in unburned carbon and iron oxides, showed no major differences. However, these differences could possibly be linked to surface-area differences. In conclusion, the much more complicated heterogeneous chemistry must be taken into consideration to get a realistic picture. When heterogeneous reaction is accounted for, particle surface area and makeup play key roles.

The importance of heterogeneous reaction implies that the use of catalysts should achieve further mercury oxidation at a commercially viable rate, thus offering a technology for mercury emission control. Several options have been explored. Kaluza and Boehm (1971) found that TiO_2 (anatase), when irradiated with ultraviolet (UV) light, would oxidize mercury vapor to mercury oxide (HgO) by producing OH radicals at the TiO_2 surface. Wu et al. (1998) aerosolized TiO_2 nanoparticles to achieve a high capture efficiency (up to 96%) of mercury vapor in combustion environments. When compared to the cost of activated carbon, they estimated that the annual cost of the photocatalytic reactor to be between $^1/_3$ and $^1/_{12}$ of the carbon. Pitoniak et al. (2003) loaded TiO_2 nanoparticles into nanostructured silica gel that required less consumption of UV light.

Other promising catalysts are Fe_2O_3 and CuO, as revealed by Ghorishi et al. (1999) and Lee et al. (2001). An addition of nitrogen dioxide (NO_2) to the base gas mixture can further enhance the oxidation capabilities. Their experiments using a synthetic fly ash (silicon dioxide [SiO_2] and aluminum oxide [Al_2O_3]) containing 14% Fe_2O_3 conducted at 250 ˚C resulted in 90% oxidation of the mercury vapor. CuO was shown to be even more capable of oxidizing mercury. Adding 1% CuO to the fly ash produced oxidation levels rivaling the 14% Fe_2O_3. The possible mechanisms for this catalytic reaction were not discussed in the paper. However, Olson et al. (1999) speculated the probable oxidation product of Hg^0 by NO_2 (over activated carbon) to be $Hg(NO_3)_2 \cdot H_2O$. Lee et al. (2001) also carried out studies on real coal fly ashes (Blacksville–high iron content and Absaloka–low iron content) with the emphasis on the iron content and the effects of NO_x, sulfur dioxide (SO_2), water (H_2O), and hydrogen chloride (HCl). The form of the iron was found to be an important factor.

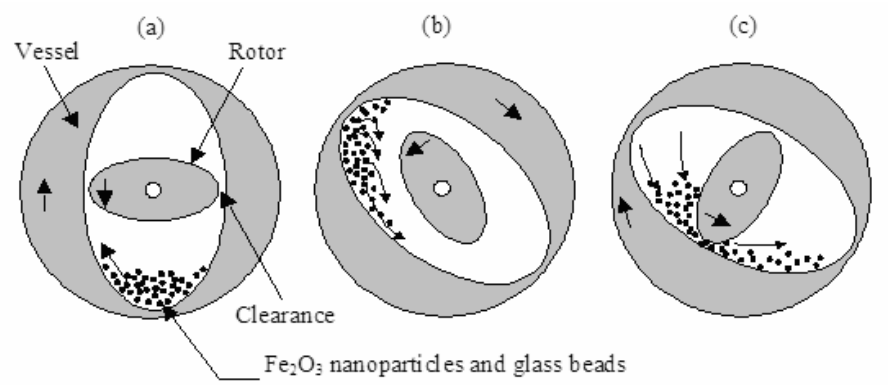

Figure 1. Mechanism of the dry mechanical particle coating process in Theta Composer.

Table 1. Properties of Fe_2O_3 nanoparticles, solid glass beads, and coated beads.

Material	Particle size	Specific surface area (m^2/g)
Fe_2O_3	3[a] nm (primary particle size)	250[a] (176[b])
Glass Beads	70[a] μm (mean)	0.035[c]
Coated Beads	70 μm (mean)	0.605[b]

a. Provided by the manufacturer

b. Measured by Nova

c. Calculated value based on external surface of a solid sphere

The non-magnetic Fe_2O_3 was found to be more reactive than the magnetic Fe_3O_4. NO_x promoted the oxidation while HCl, SO_2 and H_2O inhibited it.

While previous studies have demonstrated the potential of Fe_2O_3 in fly ash to remove mercury in flue gas, the mechanisms are not clearly known. Furthermore, the potential of the material in the nanoparticle form, which is known to have higher surface kinetics, has not been explored. The objective of this study was to examine the effectiveness and mechanisms of high surface area Fe_2O_3 nanoparticles by studying the interaction with mercury vapor without the presence of unburned carbon and fly ash. The optimal temperature will be determined as well. By doing so, the true characteristics of this material can be revealed. Understanding the mechanisms and optimal operating range of the material is the first step in exploring and developing this technology for real-world application.

2. Experimental Design

Fe_2O_3 nanoparticles (Mach I, Inc.) were coated onto glass beads (3M) using a dry coating device based on mechanofusion technique called Theta Composer (Model THC-Lab, Tokuju Corp.). Figure 1 shows a diagram of the device. The coating mechanism has been discussed in Watano et al. (2000), and hence only the key steps are described here. In this study, the vessel was rotated at 75 rpm, while

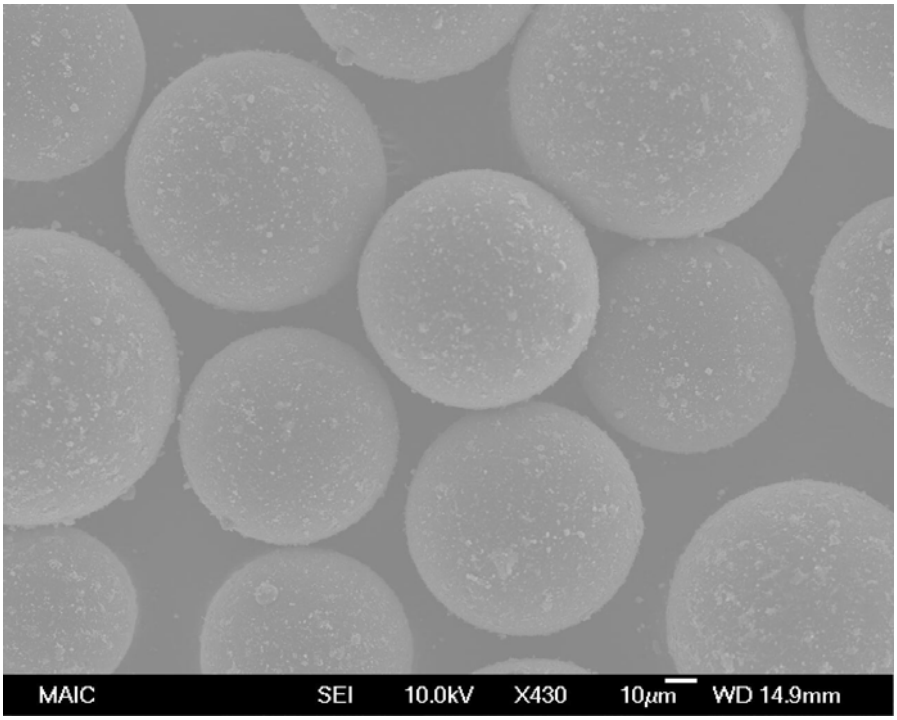

Figure 2.a

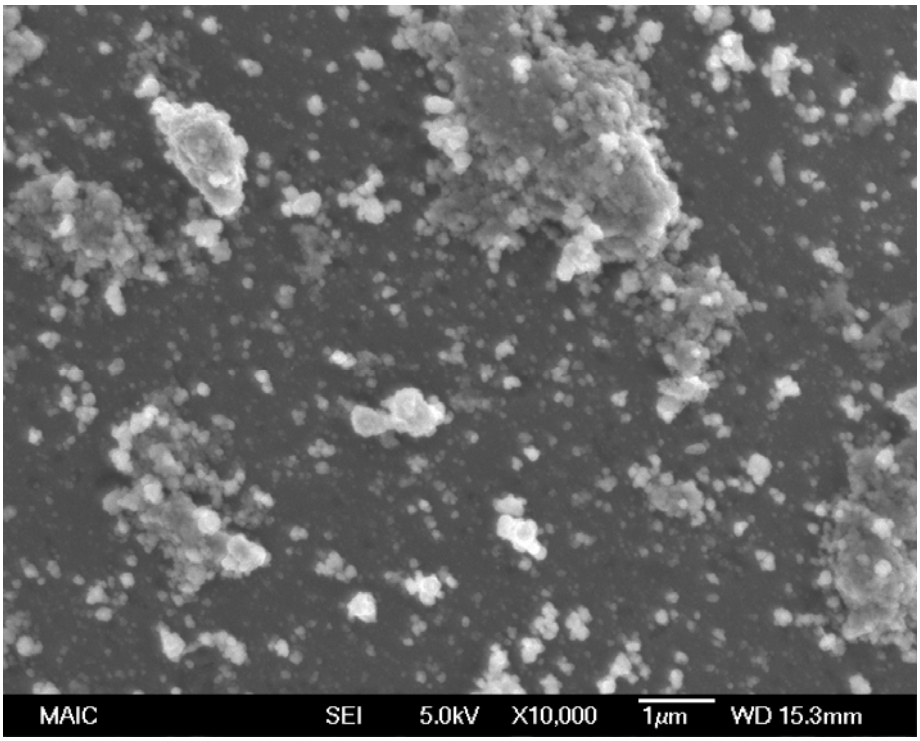

Figure 2.b

Figure 2. SEM pictures of coated beads: (a) X430 for the entire coated beads; (b) X10,000 for closer look of the coated nanoparticles on the surface.

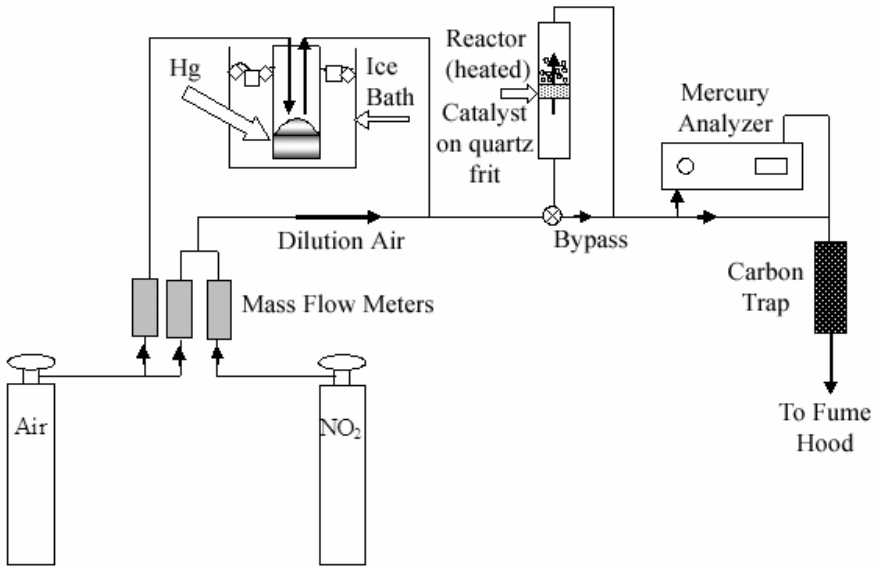

Figure 3. A schematic diagram of the experimental setup.

the rotor speed was 2500 rpm in the opposite direction for 30 minutes. The rotation forced the nanoparticles and the solid glass beads to pass through a narrow clearance between the rotor and the wall of the vessel. Nanoparticles were coated onto the glass beads due to the high sheer force experienced when they passed through the gap (i.e., configuration [c]). Table 1 shows the characteristics of the glass beads as well as the Fe_2O_3 nanoparticles. Figure 2 shows scanning electron micrographs (SEM) of the coated particles, and Figure 2a shows a fairly uniform distribution of the nanoparticle patches on the glass beads. Specific surface area measurement by the Brunauer-Emmett-Teller (BET) method (Quantachrome Nova 1200 and Quantachrome Ultrapycnometer 1000) showed an increased surface area compared to the naked beads (Table 1), due to the nanoparticle coating. The coated beads were also digested by hot nitric acid (HNO_3) (tracemetals grade, Fisher Scientific) for four hours. The acid solution was diluted and then analyzed by Inductively Coupled Plasma–Optical Emission Spectroscopy (ICP-OES, Perkin Elmer, Optima 3200 RL). The ICP-OES analysis showed that the coating percentage was 0.236%.

These coated beads were evaluated in a fixed-bed reactor system, the schematic of which is shown in Figure 3. Breathing grade air (Praxair), measuring 90 cm^3/min and controlled by a mass flow controller (FMA 5400/5500, Omega), was passed over liquid mercury in an ice-bathed reservoir, resulting in an outflow of mercury-laden air. The mercury-laden air then merged with a second stream of air, the dilution air, which flowed at 860 cm^3/min. The air with a designated mercury concentration then flowed to the reactor, which was heated to a designated temperature using heating tape, and ultimately to the Hg analyzer. The flow could also bypass the reactor and go directly to the mercury analyzer to determine the inlet Hg vapor concentration. The reactor is a 200 mm long, 25 mm outside

diameter (20 mm inside diameter) glass tube with a quartz frit in the middle (10-20 μm porosity, Ace Glass).

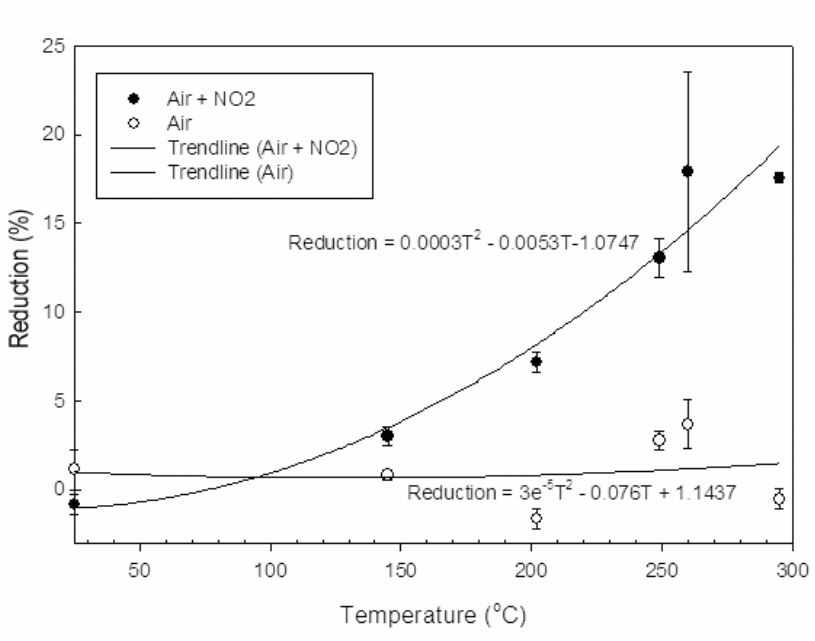

Figure 4. A scatter plot of trials (combined) to determine loss through the reactor without catalyst or beads.

The reactor was heated with heating tape wrapped along the full length of the tube. The concentrations of mercury in the air streams were monitored on-line with a mercury analyzer (VM 3000, Mercury Instruments) that is based on the absorption of 253.7 nm wavelength by elemental mercury vapor. Teflon (PTFE) tubing and stainless steel fittings were used throughout the system to avoid reaction on the tubing walls. Finally, the air stream passed through an activated carbon trap before exiting to the exhaust hood.

Four sets of experiments were carried out to assess the performance of the prepared materials, followed by material analysis. In the first set of experiments, as a control, the mercury-laden air was passed through the system without any beads to characterize the loss of Hg^0 in the system. Also in this set, experiments were run with uncoated beads to determine any possible removal by the glass beads. In the second set, experiments were conducted to determine the mechanism for the mercury removal by saturating the coated beads in air. The trials were run until the readings reached 90% of the baseline for the air-only environment. While Fe_2O_3 nanoparticles showed the capability of removing mercury in an air environment, flue gas contains many other gases that may affect the performance. One example is the addition of NO_2 to their base gas, which resulted in a high oxidation rate (Ghorishi et al., 1999). Therefore, experiments were also conducted in air with NO_2. When NO_2 (5120 ppm in N_2, Praxair) was introduced at a flow rate of 40 cm^3/min, the dilution air flow rate was reduced to 820 cm^3/min. The resultant NO_2 concentration entering the reactor was 215 ppm. In the third set, they were heated in air only and saturated several times to examine if desorption and adsorption occurred. Finally, in the fourth set, the coated beads were evaluated over a range of

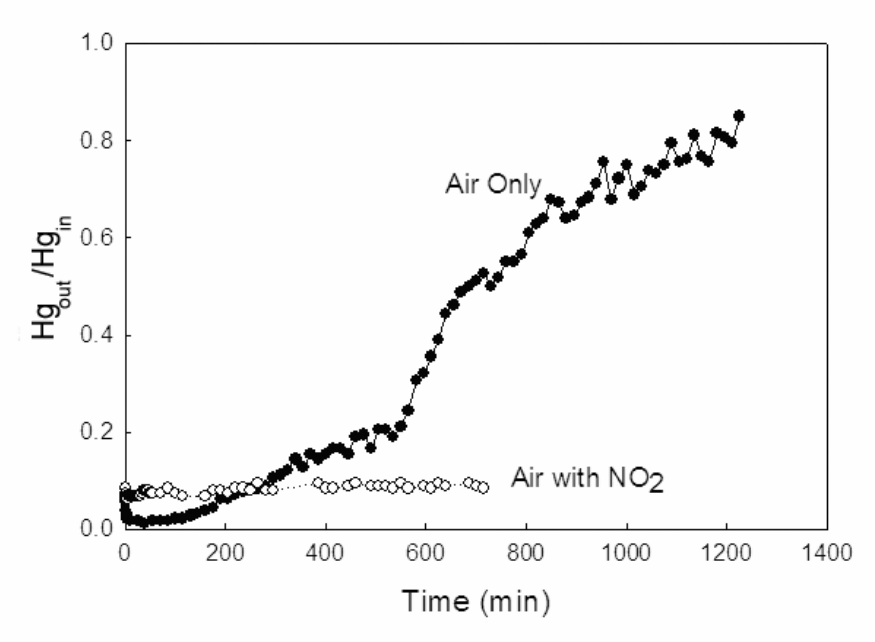

Figure 5. Representative results of saturations with 5 g of coated beads for air only and air with NO_2.

temperatures to determine the optimal temperature range of operation.

To determine the quantity of adsorbed mercury, Cold-Vapor Atomic Fluorescence Spectrometry (CV-AFS) was used. The samples were dissolved in a mixture of concentrated HNO_3 and sulfuric acid (H_2SO_4) (3:1 v/v ratio), and allowed to digest overnight at sub-boiling temperature. Following digestion, the samples were diluted, reduced with stannous chloride ($SnCl_2$) and analyzed by CV-AFS (Tekran® 2600). Samples included beads used in experimental set 2, unused coated samples, and uncoated glass beads. Quality assurance/quality control (QA/QC) criteria were met by running digestion blanks (no beads, no iron), standard reference materials, and samples spiked with known amounts of mercury.

3. Results and Discussion

Experimental Set 1

Mercury-laden air or mercury-laden air with 215 ppm NO_2 was passed through the reactor to determine the loss due to the reactor. Experiments began with a room-temperature run, followed by runs of increased temperature. Figure 4 shows a scatter plot of the percent loss of elemental mercury versus temperature. A trendline is added for air as well as for air with NO_2. The equations for the trendlines were used later to subtract the reactor loss from the observed mercury removal in the following experimental sets to determine the true effects of the nanoparticles in the reactor. As shown in Figure 4, in the presence of air only the loss was minimal throughout the temperature range. The presence of NO_2, however, resulted in the loss of elemental mercury vapor, and the loss increased as temperature increased. The observed loss agrees with earlier studies on the role of NO_2 (Hall et al.,

1995; Norton et al., 2003). The loss may be homogeneous or heterogeneous (on the porous frit surface) following the reaction pathway (Hall et al., 1995) of

$Hg + nNO_2 \rightarrow$ products (e.g. HgO + NO) (2)

The losses due to the uncoated beads in the reactor were also measured. The results were found to have no discernable differences (data not shown), demonstrating that the solid beads did not affect mercury in the system.

Experimental Set 2

To examine if catalysis is truly the mechanism as pointed out in prior studies (Ghorishi et al., 1999; Lee et al., 2001), 5 g of Fe_2O_3 nanoparticle-coated beads were placed in the reactor, and saturation of the material with mercury was attempted. This amount of material provided a bed depth of 13 mm and a contact time of only 0.25 s. Mercury-laden air (feed concentration maintained at around 18 ppb) was run through the reactor at 260 ºC, which was used in the prior studies (Ghorishi et al., 1999; Lee et al., 2001), until the concentration rose to 90% of the feed concentration. Figure 5 shows a representative result in air only. As seen, the mercury concentration dropped quickly to a minimum reading, and then gradually rose. The gradual increase of concentration indicates that the materials were acting as an adsorbent (instead of a catalyst) in the air-only system and became saturated over time. After the trials, the particles were salvaged to determine if mercury was adsorbed on them, the results of which will be discussed later. Clearly demonstrated is the feasibility of this material for high removal efficiency as an adsorbent. With a bed depth of 3 mm, the material had a remarkable efficiency for over 100 minutes.

Also shown in Figure 5 is the result for 5 g of coated beads in air with 215 ppm NO_2. A very interesting phenomenon that differed from the air only test was observed. Unlike the experiments with air only, the mercury concentration remained constant for the entire 700 minutes, showing no sign of saturation. This indicated that in the presence of NO_2, the particles were acting as a catalyst, as suggested by Ghorishi et al. (1999) and Lee et al. (2001), rather than an adsorbent. After the experiments, the material was also analyzed by CV-AFS to determine the amount of mercury on the particles. It should be emphasized that excellent removal of mercury vapor was observed over 700 minutes without any diminishing performance. The different roles that the material plays under different scenarios have not been reported in previous studies. Results from the current study show that the improved removal is possibly attributed to the catalytic effects of the Fe_2O_3 in the presence of NO_2. Identifying the mechanisms under various conditions is critical to how the material can be applied to practical systems.

Experimental Set 3

The goal of this set of desorption and re-saturation experiments was to verify whether mercury was adsorbing and desorbing to the Fe_2O_3 nanoparticles. Materials used in the previous saturation

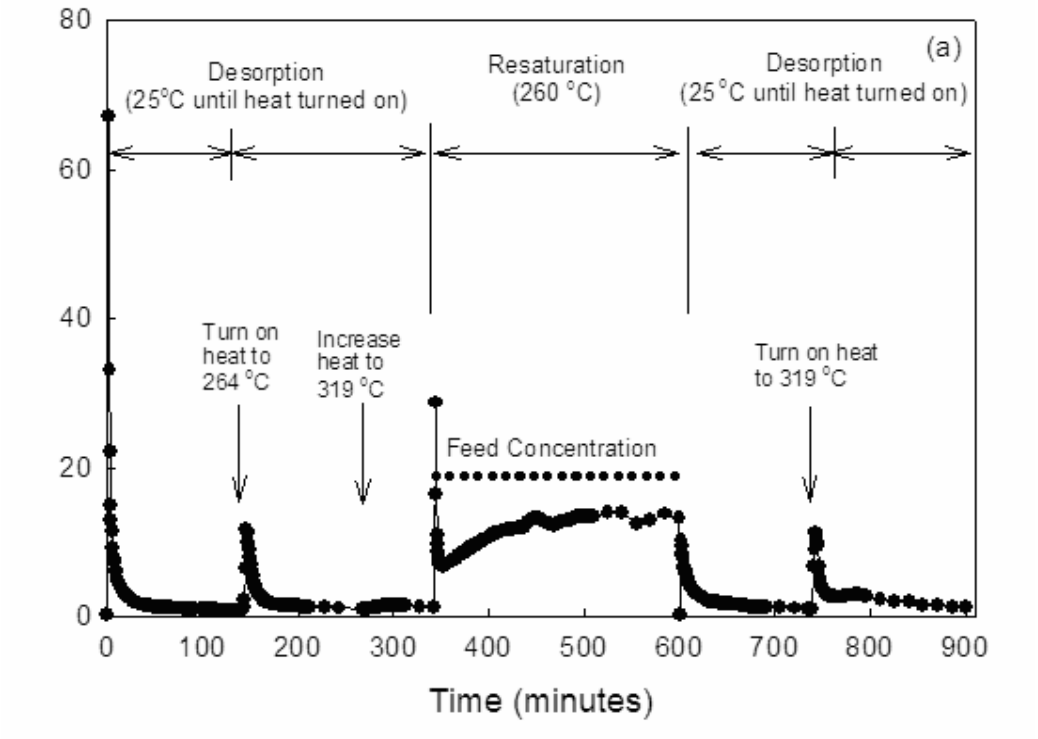

Figure 6.a

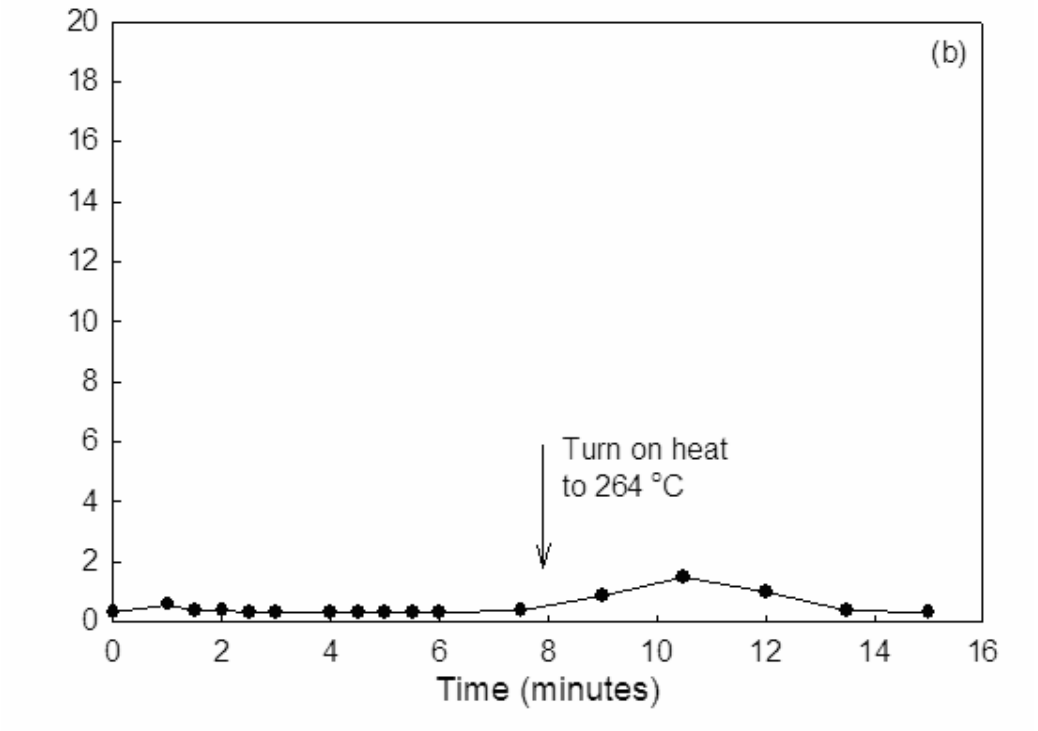

Figure 6.b

Figure 6. (a) Desorption of saturated Fe_2O_3 catalyst in air only, followed by re-saturation, and re-desorption; (b) desorption of Fe_2O_3 catalyst that was used in experimental set 2 with air and NO_2.

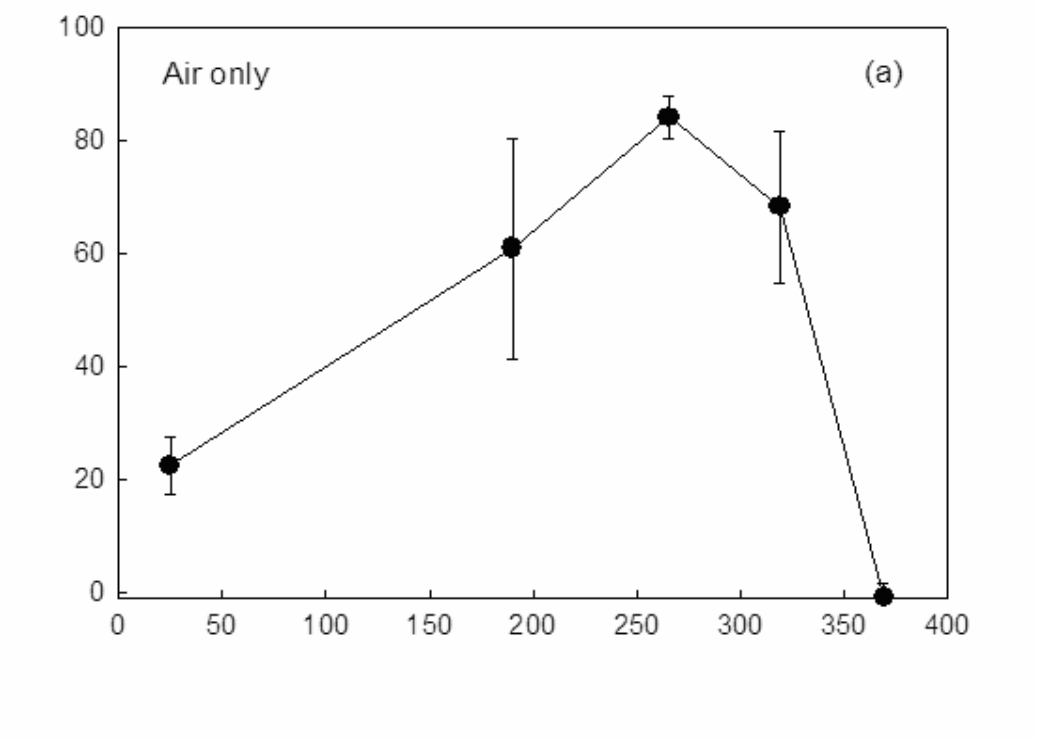

Figure 7.b

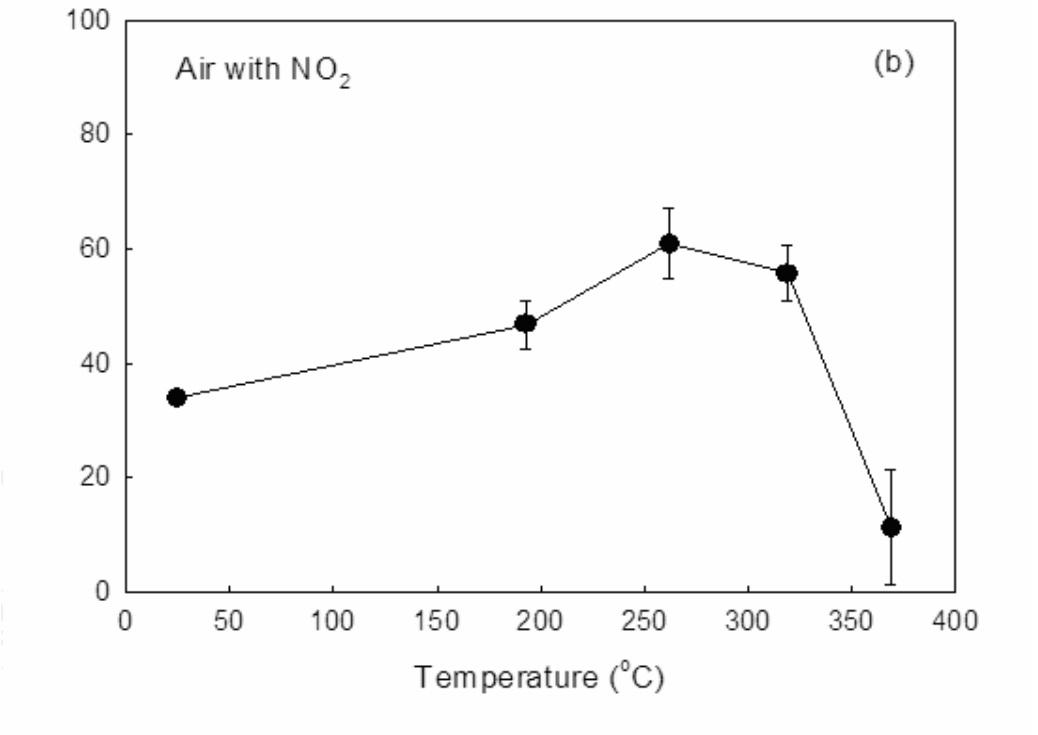

Figure 7.b

Figure 7. (a) Removal efficiency at 20 minutes as a function of temperature for air only; (b) removal efficiency as a function of temperature in air with NO_2. Note that the reactor losses (Figure 4) have been subtracted.

experiments were subjected to desorption, resaturation, and desorption again. Figure 6a shows the results for tests in air only. The first desorption was run at room temperature with air only until it dropped below 1.0 ppb. Clearly observed was a spike of elemental mercury concentration, showing the release of adsorbed mercury from the material. The heating tape was then turned on to 264 ^{o}C to see if more mercury would be desorbed, and mercury desorption was indeed observed. When the reading reached 1.0 ppb again, the temperature was further raised to 319 ºC. However, this time further desorption was negligible.

The material was then re-saturated by following the same procedure as in set 2. In the second saturation, however, the concentration never dropped below 6.8 ppb, and it rose gradually to around 13 ppb after 360 minutes. The material then underwent the second phase of desorption. The results were similar to the first desorption (i.e., mercury was desorbed from the material). In this desorption, the temperature was set to 319 ºC instead of using the two-step procedure of the first desorption. The spike when the heat was first turned on reached a level similar to that of the first desorption. The fact that the spike occurred when the heat was applied, along with the fact that the concentration decreased over time during desorption, indicate that mercury is being physically adsorbed in the system and that this mercury can be desorbed. The ability to desorb mercury means that the material can be reused.

Figure 6b shows the desorption result for the materials used in the air with NO_2 test. The elemental mercury vapor concentration remained very low during the entire desorption phase, i.e. the data showed very little indication of mercury being desorbed from the particles. This result further supports that the presence of NO_2 causes the Fe_2O_3 nanoparticles to become a catalyst, rather than an adsorbent.

Experimental Set 4

The coated beads were placed in the reactor with each run conducted at an increasingly higher temperature to determine the effective temperature range. Since the material gradually saturated over time in air only as discovered in set 2, the removal efficiency at 20 minutes versus the temperature are presented in Figure 7a, with the control results (Figure 4) subtracted. As shown, each end of the temperature range had almost no reduction in mercury vapor concentration. However, in the range of about 180 to 320 °C, there was a strong reduction (~85% at 260 °C). Figure 7b shows the efficiency versus temperature of the air with NO_2 with the control results (Figure 4) subtracted. The results for the 215 ppm NO_2 also show an ideal temperature of about 260°C, with a range similar to that of air only. At room temperature, the material is not well activated, and the material's capability increases as temperature increases. At temperatures above the range, elemental vapor is the thermodynamically favored species (Wu and Biswas, 1993). Hence, the removal efficiency dropped at high temperature. Because of the two different removal mechanisms present depending on the presence or absence of NO_2, it should be noted that the efficiencies of air only and air with NO_2 should not be directly compared.

This result shows that there is a temperature window of application, and indeed an optimal temperature for the use of the catalyst. This identified temperature agrees with the one that Ghorishi et al. (1999) and Lee et al. (2001) used in their experiments. Identifying the temperature window provides critical information to users of practical applications.

Table 2. Results for atomic fluorescence spectrometry, along with calculated theoretical specific capacities.

Sample	Specific capacity (μg/g Fe_2O_3) by AFS	Specific capacity (μg/g Fe_2O_3) by calculation
Sample 1 (air only)	226 (±57)	1526
Sample 2 (air only)	451 (±61)	914
Sample 3 (air only)	467 (±285)	1727
Sample 4 (air + NO_2)	63 (±16)	NA

Adsorption Capacity

Because the specific removal capacity relates to any sorbent material application, it was estimated from the area between the feed line and the outlet concentration over the entire test period. The area was then multiplied by the flow rate to arrive at the total amount of mercury being adsorbed. This number was divided by the amount of iron (determined by ICP-OES measurements) to determine the specific capacity. The specific capacities estimated for three tests in set 2 using 1.15 g of material are listed in Table 2. The range of obtained values is similar to those reported in the literature for common carbons (Brown et al., 1999).

These materials were acid digested and the concentrations were measured by CV-AFS. The results are presented in Table 4. The measured specific capacities for air only (samples 1-3) are lower than the calculated values. As demonstrated in experimental set 3, some mercury readily desorbed from the Fe_2O_3. Therefore, some of the mercury was possibly lost in activities prior to digestion and CV-AFS detection. This property resulted in the wide variation in the measured capacity. The specific capacity for the air-with-NO_2 sample (sample 4) was low, indicating that little mercury was adsorbed. The results of the AFS further substantiate the hypothesis that in the presence of air only, the particles are physically adsorbing the mercury, while in the presence of NO_2, the conversion is more catalytic in nature. Also, in the presence of NO_2 the oxidized mercury is not associated with the particles, and therefore must remain in the air stream. There may be two advantages associated with this result. First, oxidized mercury has a higher affinity with particles in flue gas and has better solubility. This would allow for the removal of the oxidized mercury downstream by scrubbers or other conventional particulate control devices. Second, the fact that Fe_2O_3 is not loaded/saturated by mercury would allow for the continual use of the Fe_2O_3 nanoparticles in the system, rather than just for disposal.

NO_2 has important and interesting effects in relation to Fe_2O_3 nanoparticles. Indeed, Fe_2O_3 thin

film and nanoparticles have been used as a NO_2 sensor due to its NO_2 adsorption capability (Yamazoe and Miura, 1994; Sun et al., 1995; Neri et al., 2002). Hence, it can also be hypothesized that elemental mercury removal in the presence of NO_2 results from co-chemisorption of mercury and NO_2 on Fe_2O_3 nanoparticles. However, the potential products (e.g., $Hg(NO_3)_2$) (Olson et al., 1999) are probably not stable on the material at the testing temperature, even if co-chemisorption does occur. Thus, the oxidized mercury subsequently vaporizes and stays in the gas phase. This agrees with the AFS results that little mercury remained on the material. It also agrees with observations in Olson et al. (1999) that oxidized mercury was emitted from their sorbent tested in a gas stream containing NO_2.

To verify whether oxidized mercury can stay in the air stream, the vapor pressure of HgO was calculated using STANJAN (Reynolds, 1995) with the thermodynamic data obtained from JANAF Thermochemical Tables (Chase et al., 1986). The resulting equation, following the Antoine format, is

$$\log_{10} P = -\frac{6840.8}{T} + 8.5604 \tag{3}$$

where P is pressure (atm) and T is temperature (K). At 260 ^{o}C (533 K), HgO vapor pressure is 5.32×10^{-5} atm (53,200 ppb), which is greater than the feed concentration of 18 ppb. Hence, the newly formed HgO tends to stay in the gas phase. When the system temperature decreases to 100 ^{o}C (373 K), the vapor pressure is lowered to 0.17 ppb. In this case, the majority of HgO has condensed. On the other hand, the vapor pressure of the volatile Hg at 100 ^{o}C is still 4.48×10^{5} ppb (Weast et al., 1983). Thus, any Hg vapor still tends to stay in the gas phase.

4. Conclusions

Effective control of mercury emission from combustion sources is an important issue. Mercury released into the environment is transformed into methyl-Hg, which bio-accumulates and ends up in high enough concentrations in fish to be dangerous to humans. The U.S. EPA has proposed a limit of effluent mercury, which will reduce mercury releases by 69% by 2018 (U.S. EPA, 2004a). The proposed Clear Skies legislation would cap emissions at 26 tons per year by 2010 and 15 tons per year by 2018 (current emissions are about 48 tons per year; U.S. EPA, 2003). To reach these regulations, many users plan to use activated carbon. However, there are alternatives that could prove to be less expensive.

In this study, Fe_2O_3 nanoparticles were used to remove elemental mercury vapor without the presence of fly ash. The mercury removal mechanisms by Fe_2O_3 nanoparticles were identified. The experimental results show that in the presence of air, the Fe_2O_3 nanoparticles act as an adsorbent of elemental mercury vapor. However, when NO_2 is present, the particles become a catalyst rather than an adsorbent that does not get saturated or breakthrough. The specific removal capacity of the particles, which averaged ~1390 μg/g, was determined for the adsorbent case. This study also identified a temperature range of 180 to 320 ºC in which to apply Fe_2O_3 nanoparticles, with an

optimal at around 260 ºC. This important finding gives a potential user the right location to place/inject the material in the flue gas system to achieve maximum results. Overall, the results demonstrate the potential of using Fe_2O_3 nanoparticles as an alternative to activated carbon and other techniques for mercury removal from combustion sources.

Acknowledgements

The authors want to acknowledge Tokuju Corp for providing the Theta Composer and Mach 1 Inc. for providing the Fe_2O_3 nanoparticles free of charge. They are very grateful to Dr. Dale Lundgren at the University of Florida and Dr. Satoru Watano at Osaka Prefecture University for insightful discussions, Mr. Gill Brubaker at Particle Engineering Research Center (PERC) for ICP analysis, and Dr. Kerry Siebein at PERC for SEM images. Scott Borderieux is very grateful to the CDM fellowship and EPA Air Pollution Training Scholarship.

References

Bergström, J. G. T. (1986) Mercury Behaviour in Flue Gases. *Waste Manage. Res.* **4:** 57-64.

Brown, T. D., Smith, D. N., Hargis, R. A., O'Dowd, W. J. (1999) Mercury Measurement and Its Control: What We Know, Have Learned and Need to Further Investigate. *J. Air Waste Manage. Assoc.* **49(6):** 628-640.

Chase, M. W., Davies, C. A., Downey, J. R., Frurip, D. J., McDonald, R. A. and Syverud, A. N. (1986) *JANAF Thermochemical Tables, 3rd Edition*, American Chemical Society and American Institute of Physics for the National Bureau of Standards, Midland, MI.

Fujiwara, N., Fujita, K., Tomura, K., Moritomi, H., Tuji, T., Takasu, S., and Niksa, S. (2002) Mercury Transformations in the Exhausts from Lab-Scale Coal Flames. *Fuel* **81:**2045-2052.

Ghorishi, S. B., Lee, C. W. and Kilgroe, J. D. (1999) Mercury Speciation in Combustion Systems: Studies with Simulated Flue Gases and Model Fly Ashes, *Proc. 92nd Annual Meeting and Exhibition of Air Waste Management Assoc.* St. Louis, MO, Paper No. 99-651.

Haberland, H., Von Issendorff, B., Yufeng, J., Kolar, T. and Thanner, G. Z. (1993) Ground State and Response Properties of Mercury Clusters. *J. Phys. D.* **26:** 8-12.

Hall, B., Schager, P., and Lindqvist, O. (1991) Chemical Reactions of Mercury in Combustion Flue Gases. *Water, Air, Soil Pollut.* **56:** 3-14.

Kaluza, U. and Boehm, H. P. (1971) Titanium Dioxide Catalyzed Photooxidation of Mercury. *J. Catal.* **22:** 347-358.

Krishnan, S. V., Gullett, B. K. and Jozewicz, W. (1994) Sorption of Elemental Mercury by Activated Carbons *Environ. Sci. Technol*. **28:** 1506-1512.

Lee, C. W., Srivastava, R. K., Ghorishi, S. B. and Kilgroe, J. D. (2001) Effects of Iron Content in Coal Combustion Fly Ashes on Speciation of Mercury, *Proc. 94th Annual Meeting and Exhibition*

of Air Waste Manage. Assoc. Orlando, FL, Paper No. 156.

Lee, T. G., Hedrick, E. and Biswas, P. (2002) Hg Reactions in the Presence of Chlorine Species: Homogeneous Gas Phase and Heterogeneous Gas-Solid Phase *J. Air Waste Manage. Assoc.*, **52**: 1316-1323.

Meij, R. (1991) The Fate of Mercury in Coal-Fired Power Plants and the Influence of Wet Flue-Gas Desulphurization. *Water, Air, Soil Pollut*. **56:** 21-33.

Neri, G., Bonavita, A. Galvagno, S. Siciliano, P. and Capone, S. (2002) CO and NO_2 Sensing Properties of Doped-Fe_2O_3 Thin Films Prepared by LPD. *Sens. Actuators, B.* **82(1)**: 40-47.

Niksa, S., Helble, J. J. and Fujiwara, N. (2001) Kinetic Modeling of Homogeneous Mercury Oxidation: The Importance of NO and H_2O in Predicting Oxidation in Coal-Derived Systems *Environ Sci. Technol*. **35**: 3701-3706.

Niksa, S., Fujiwara, N., Fujita, Y., Tomura, K., Moritomi, H., Tuji, T., and Takasu, S. (2002) A Mechanism for Mercury Oxidation in Coal-Derived Exhausts. *J. Air Waste Manage. Assoc.*, **52**: 894-901.

Norton, G. A., Yang, H., Brown, R. C., Laudal, D. L., Dunham, G. E. and Erjavec, J., "Heterogeneous Oxidation of Mercury in Simulated Post Combustion Conditions", *Fuel*, **82**, 107-116, 2003.

Olson, E. S., Sharma, R. K., Miller, S. J., Dunham, G. E. (1999) Identification of the Breakthrough Oxidized Mercury Species from Sorbents in Flue Gas. *Mercury in the Environment: Proceedings of an Air Waste Management Association Specialty Conference*, September 15-17, 1999, Bloomington, MN, pp 121.

Otani, Y., Emi, H., Kanaoka, C., Uchijima, I. and Nishino, H. (1988) Removal of Mercury Vapor from Air with Sulfur-Impregnated Adsorbents. *Environ. Sci. Technol*. **22:** 708-711.

Pitoniak, E., Wu, C. Y., Londeree, D., Mazyck, D., Bonzongo, J.-D., Powers, K. and Sigmund, W. (2003) Nanostructured Silica-Gel Doped with TiO_2 for Hg Vapor Control. *J. Nanopart. Res.*, **5(3-4)**: 281-292.

Reynolds, W. C. (1995) *STANJAN-Interactive Computer Programs for Chemical Equilibrium Analysis.* Department of Mechanical Engineering, Stanford University.

Senior, C. L., Sarofim, A. F., Zeng, T., Helble, J. J. and Mamani-Paco, R. (2000) Gas-Phase Transformations of Mercury in Coal-Fired Power Plants. *Fuel Process Technol.* **63:** 197-213.

U.S. EPA (U.S. Environmental Protection Agency) (1997) Mercury Study Report to Congress *U.S. Government Printing Office*, Washington, D.C.

U.S. EPA (U.S. Environmental Protection Agency) (2003) Section-By-Section Summary of the Clear Skies Act of 2003, *http://www.epa.gov/clearskies/section-by-section_summary.pdf* (accessed November 2003).

U.S. EPA (U.S. Environmental Protection Agency) (2004a) What You Need to Know about Mercury in Fish and Shellfish. *http://www.epa.gov/ost/fishadvice/advisory.pdf* (accessed March 24, 2004).

U.S. EPA (U.S. Environmental Protection Agency) (2004b) Summary of Proposed Options to Significantly Reduce Mercury Emissions from Electric Utilities

http://www.epa.gov/mercury/mercuryfact12-15final.pdf, (accessed January 2004).

Watano, S., Imada, Y., Miyanami, K., Wu, C. Y., Dave, R. N., Pfeffer, R and Yoshida, T. (2000) Surface Modification of Food Fiber by Dry Particle Coating. *J. Chem. Eng. Jpn.* **33(6):** 848-854.

Weast, R. C., Astle, M. J. and Beyer, W. H. (Eds.) (1983) CRC Handbook of Chemistry and Physics, 64th Edition, *CRC Press, Inc.*, Boca Raton, FL, p. D-216.

Wu, C. Y. and Biswas, P. (1993) An Equilibrium Analysis to Determine the Speciation of Metals in an Incinerator. *Combust. Flame.* **93**: 31-40.

Wu, C. Y., Lee, T. G., Tyree, G., Arar, E. and Biswas, P. (1998) Capture of Mercury in Combustion Environments by *In-Situ* Generated Titania Particles with UV Radiation. *Env. Eng. Sci*. **15(2)**: 137-148.

Yamazoe, N. and Miura, N. (1994) Environmental Gas Sensing. *Sens. Actuators, B.* **20(2-3)**: 95-102.

Zeng, H., Jin, F. and Guo, J. (2004) Removal of Elemental Mercury from Coal Combustion Flue Gas by Chloride-Impregnated Activated Carbon. *Fuel*, **83:** 143-146.

Received for review, April 9, 2004
Accepted, May 2, 2004